Electronic Supplementary Information

Heat and osmosis cooperatively driven power generation in robust two-dimensional hybrid nanofluidic channels

Tianliang Xiao, Xuejiang Li, Zhaoyue Liu, Bingxin Lu, Jin Zhai* and Xungang Diao**

Content:

11. Numerical simulations of heat and osmosis cooperatively driven power generation (Figure S10).

12. The simulated current, anion current and cation current of different surface charge density (Figure S11).

13. The simulated *I-V* curves of different temperature gradient (Figure S12).

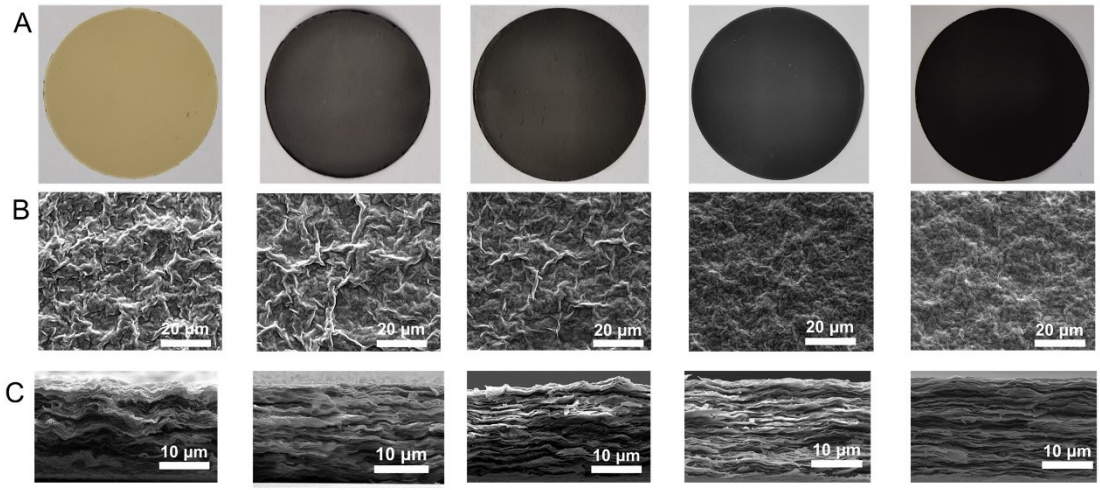

Figure S1. The optical photographs (A), the SEM imges of surface (B) and cross section (C) of MMT, MG-75%, MG-50%, MG-25 and GO nanochannel membranes.

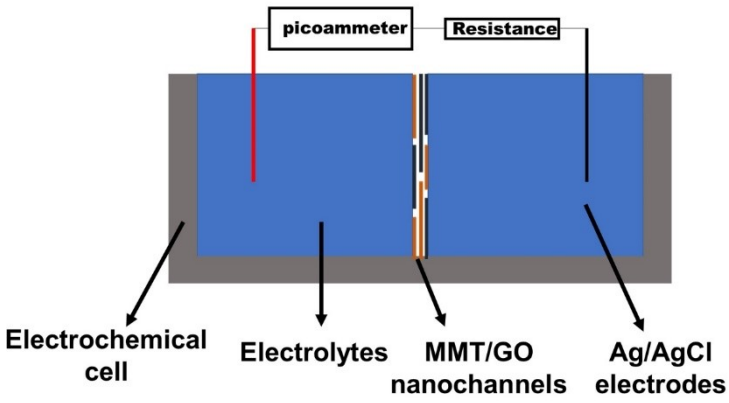

Figure S2. Schematic setup of the energy conversion device. The nanochannel membranes were placed in the middle of an electrochemical cell. The two chambers were filled with electrolytes of different concentration and temperature, which were connected with Ag/AgCl electrodes.

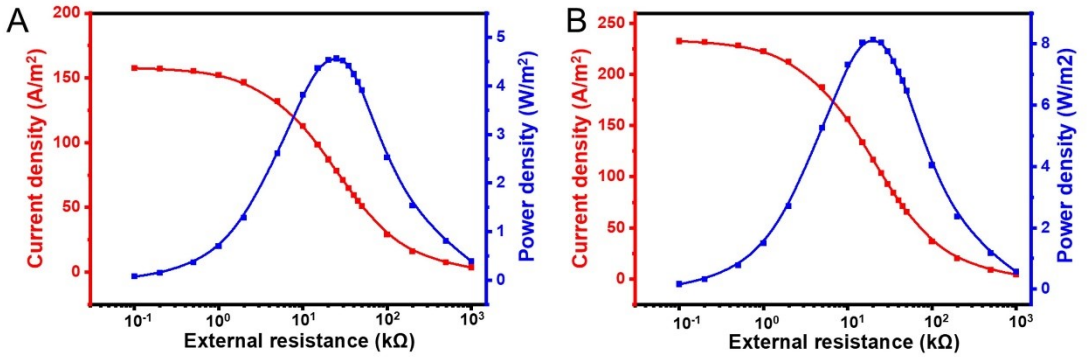

Figure S3. The current density and power density of MMT nanochannel membrane with 50-fold salinity gradient (A) and 50-fold salinity gradient coupled with 30 °C temperature gradient (B).

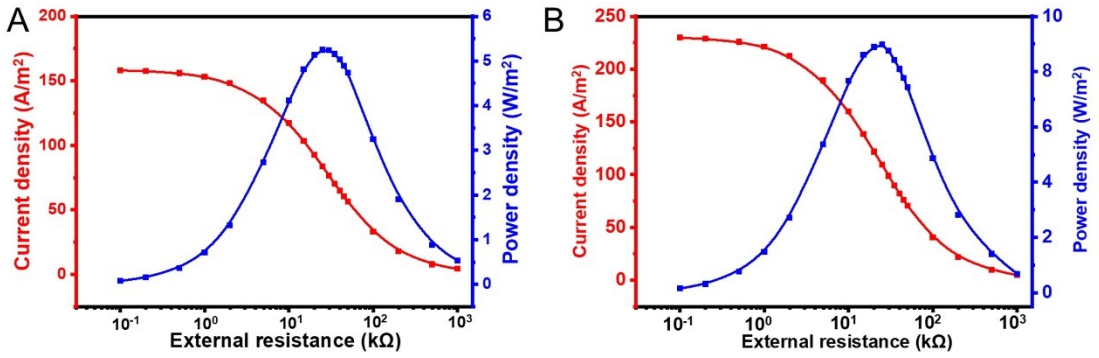

Figure S4. The current density and power density of MG-75% nanochannel membrane with 50-fold salinity gradient (A) and 50-fold salinity gradient coupled with 30 °C temperature gradient (B).

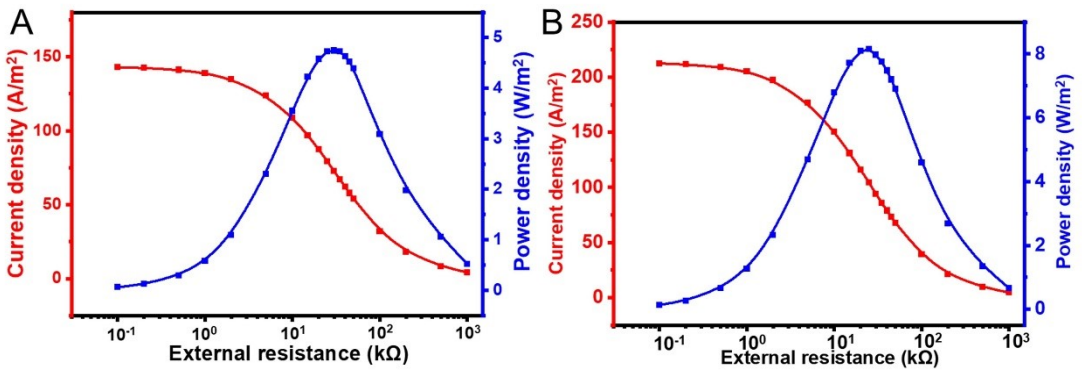

Figure S5. The current density and power density of MG-50% nanochannel membrane with 50-fold salinity gradient (A) and 50-fold salinity gradient coupled with 30 °C temperature gradient (B).

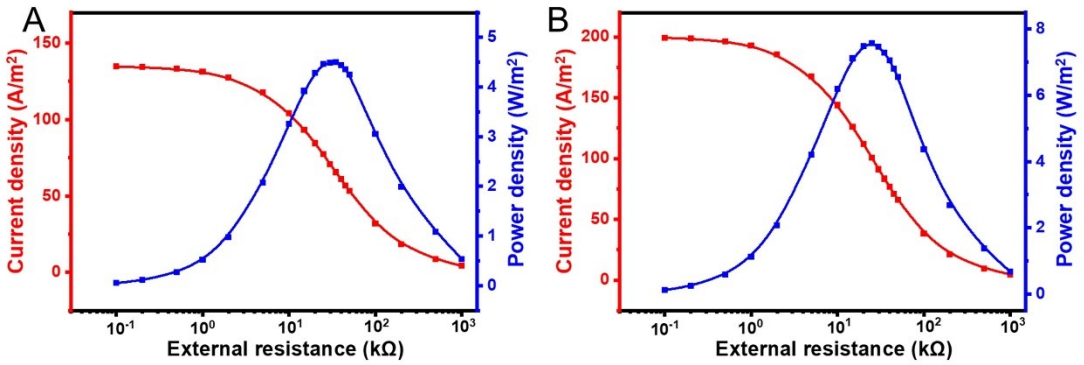

Figure S6. The current density and power density of MG-25% nanochannel membrane with 50-fold salinity gradient (A) and 50-fold salinity gradient coupled with 30 °C temperature gradient (B).

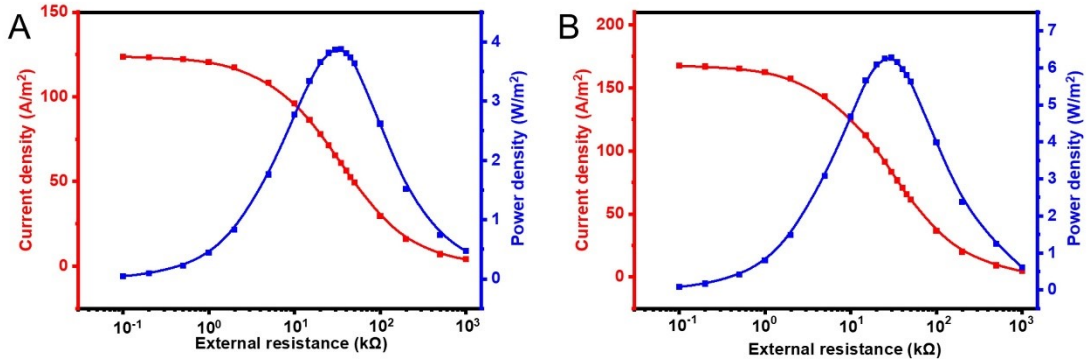

Figure S7. The current density and power density of GO nanochannel membrane with 50-fold salinity gradient (A) and 50-fold salinity gradient coupled with 30 °C temperature gradient (B).

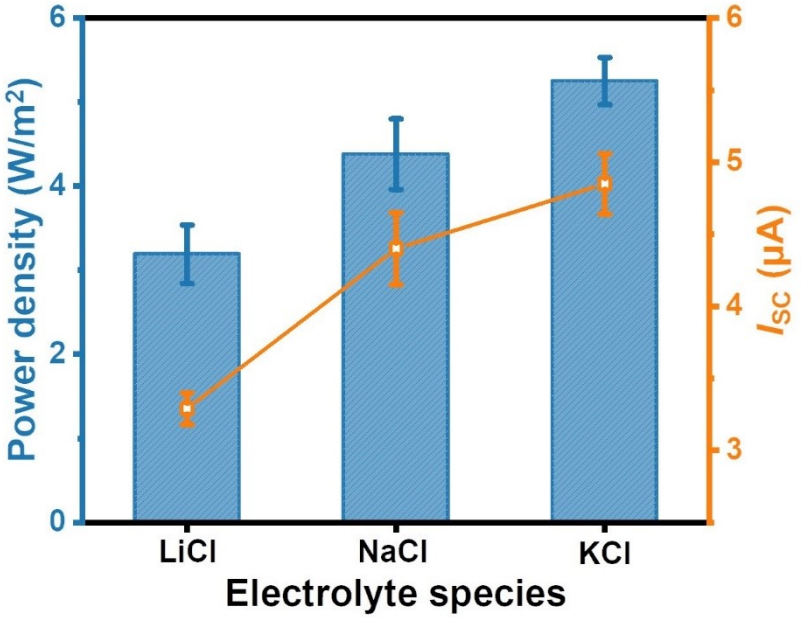

Figure S8. The power density and I_{SC} of MG-75% nanochannels in 50-fold electrolytes with different cations (LiCl, NaCl and KCl).

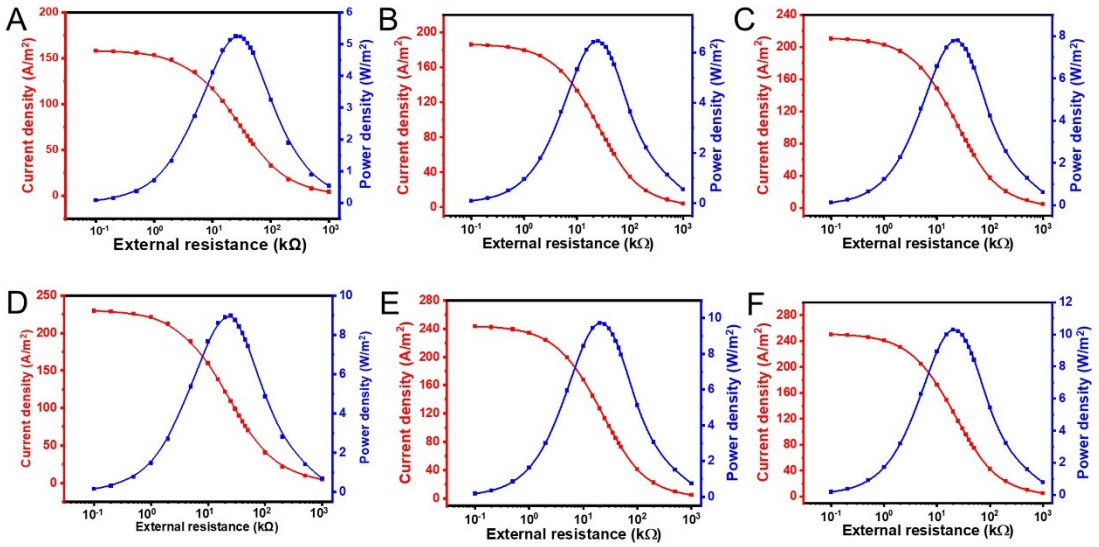

Figure S9. The current density and power density of MG-75% nanochannel membrane with 50-fold salinity gradient coupled with temperature gradient of 0 °C (A), 10 °C (B), 20 °C (C), 30 °C (D), 40 °C (E) and 50 °C (F).

Table S1. The comparison of power density among proposed hybrid nanofluidic channels and state-of-the-art 2D nanochannels.

Nanochannels	Salinity Gradient	Temperature	Power density (W/m^2)	Year	Ref.
black phosphorus/GO	50	298 K	3.4	2020	S1
GO/CNFs	50	323 K	7.2	2020	S2
GO/SNFs/GO	50	313 K	9.0	2020	S3
oppositely charged MXene	50	298 K	4.6	2020	S4
MoS_2/CNFs	50	298 K	5.2	2021	S5
GO/ANFs	50	298 K	5.06	2021	S6
vermiculite	50	298 K	4.5	2021	S7
GO/AAO	50	298 K	3.73	2021	S8
MXene/BN	50	336 K	6.2	2021	S9
MXene/PS-b-P2VP	50	298 K	6.74	2021	S10
heterogeneous MXene	50	298 K	8.6	2022	S11
bsGOMs	50	298 K	5.5	2022	S12
CNC/GO	50	337 K	10.92	2022	S13
MXene/GO	50	343 K	7.88	2022	S14
heterogeneous MMT	50	298 K	2.1	2022	S15
MMT/ANFs	50	323 K	6.45	2022	S16
MMT	50	293 K/323 K	8.53	2022	S17
GO/PDA	50	298 K	3.3	2023	S18
This work (MMT/GO)	50	293 K/343 K	10.29		

Numerical simulations

The ion transport properties were quantitatively investigated using "Electrostatics", "Transport of Diluted Species", "Single-Phase Laminar Flow" and " Heat Transfer in Fluids" modules in COMSOL Multiphysics 5.6. To simplify the calculation, the 2D nanochannel membrane was theoretically modeled as a 600-nm-length (L) cylindrical nanochannel with 4-nm width (d) (Figure S9). c_H and c_L refer to the electrolyte concentration of high side and low side, respectively. T_H and T_L refer to the temperature of high and low electrolyte concentration side, respectively ($\Delta T = T_L - T_H$). The calcualtion was based on the Poisson-Nernst-Planck equations, the steady state continuous equations and Einstein-Stokes equations as shown below:

$$\nabla^2\phi = -\frac{F}{\varepsilon}\sum z_i c_i$$

$$J_i = -D_i\left(\nabla c_i + \frac{z_i F c_i}{RT}\nabla\phi\right)$$

$$\nabla J_i = 0$$

$$D_i = \frac{k_B T}{6\pi\eta r}$$

φ, ε, z_i, c_i, J_i and D_i denote electrical potential, the dielectric constant of medium, the charge number, the ionic concentration, the ionic flux and the diffusion coefficient of each species i, respectively. T, F, R, k_B, η and r are the absolute temperature, Faraday constant, universal gas constant, Boltzmann constant, the dynamic fluid viscosity of water and the ion size, respectively. The boundary conditions of the nanochannel are as follows:

$$\vec{n}\cdot\nabla\phi = -\frac{\sigma}{\varepsilon}$$

$$\vec{n}\cdot J_i = 0$$

$\vec{n}$ represents the unit normal vector.

The ionic current of species i can be calculated by integrating the ionic flux along the cross section of the nanochannel:

$$I_i = \int_s J_i ds = -\int_s D_i(\nabla c_i + \frac{z_i F c_i}{RT}\nabla\phi) ds$$

The cation transference number (t_+) can be obtained by:

$$t_+ = \frac{|I_p|}{|I_p| + |I_n|}$$

I_p and I_n refer to the cation current and anion current, respectively.

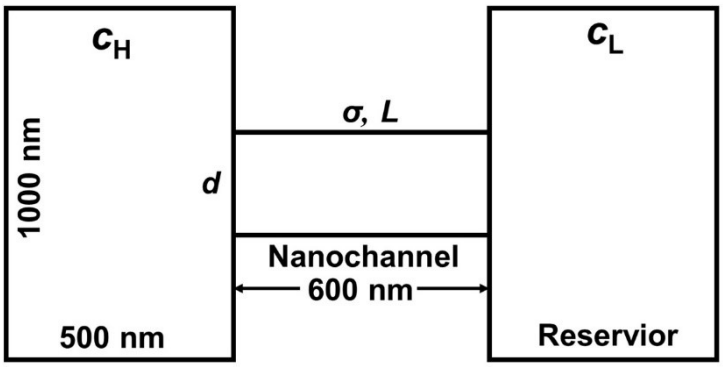

Figure S10. Theoretical model of the 2D nanochannels.

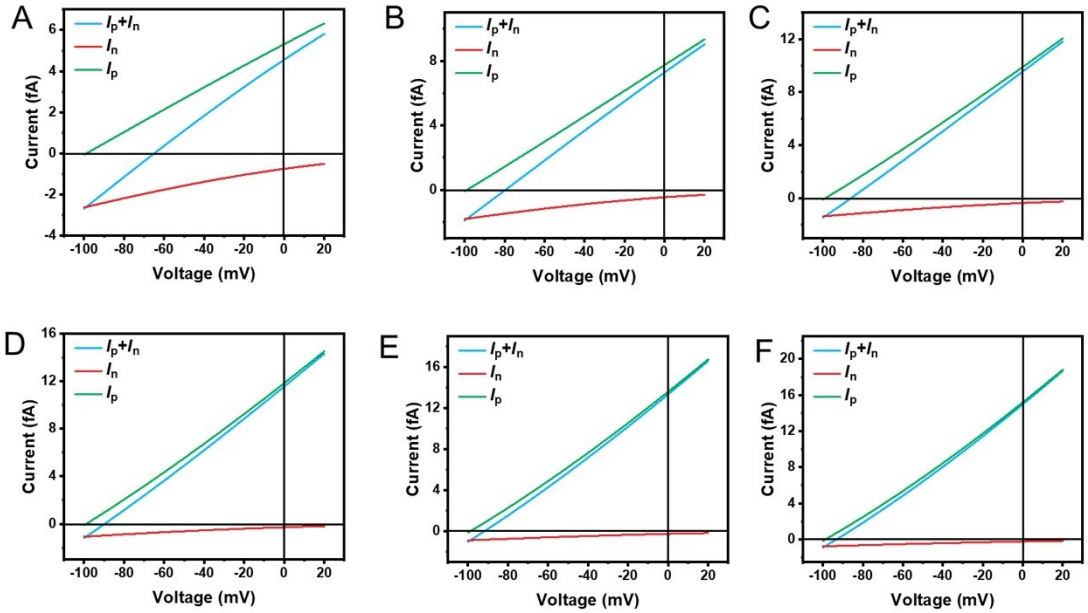

Figure S11. The simulated current, anion current and cation current by adjusting the surface charge density of the nanochannel from -1 to -6 mC/m^2 under 50-fold salinity gradient and 30 °C temperature gradient.

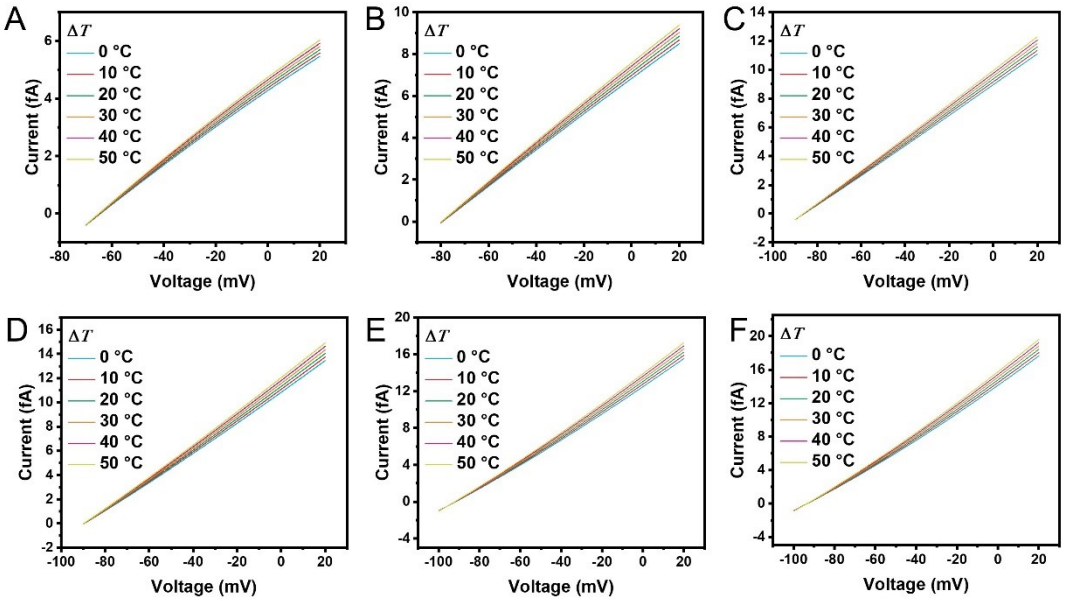

Figure S12. The simulated *I-V* curves with the surface charge density of -1 to -6 mC/m^2 (A-E) under ΔT from 0 to 50 °C.

References

[1] Z. Zhang, et al. Proc. Natl. Acad. Sci. 117 (2020) 13959-13966.

[2] Y. Wu, et al. Mater. Horiz. 7 (2020) 2702-2709

[3] W. Xin, et al. ACS Nano 14 (2020) 9701-9710.

[4] L. Ding, et al. Angew. Chem. Int. Ed. 59 (2020) 8720-8726.

[5] C. Zhu, et al. J. Am. Chem. Soc. 143 (2021) 1932-1940.

[6] J. Chen, et al. ACS Cent. Sci. 7 (2021) 1486-1492.

[7] L. Cao, et al. J. Mater. Chem. A 9 (2021) 14576-14581.

[8] L. Zhang, et al. Small 17 (2021) e2100141.

[9] G. Yang, et al. ACS Nano 15 (2021) 6594-6603.

[10] X. Lin, et al. Adv. Funct. Mater. 31 (2021).

[11] L. Ding, et al. Angew. Chem. Int. Ed. 61 (2022) e202206152.

[12] Y. Qian, et al. J. Am. Chem. Soc. 144 (2022) 13764-13772.

[13] W. Zhao, et al. Nano Energy 98 (2022) 107291.

[14] F. Wang, et al. J. Membr. Sci. 647 (2022) 120280.

[15] J. Hao, et al. Electrochim. Acta 423 (2022) 140581.

[16] R. Qin, et al. Nano Energy 100 (2022) 107526.

[17] T. Xiao, et al. Nano Energy 103 (2022) 107782.

[18] J. Hao, et al. J Colloid. Interface Sci. 630 (2023) 795-803.